

4. CAUSE OF THE MIDDLE/LATE MIOCENE CARBONATE CRASH: DISSOLUTION OR LOW PRODUCTIVITY?¹

Shijun Jiang,² Sherwood W. Wise, Jr.,² and Yang Wang²

ABSTRACT

The middle/late Miocene “carbonate crash,” a sharp decrease in carbonate mass accumulation rates in the eastern and central equatorial Pacific, as well as the Caribbean region, has previously been considered only a dissolution event associated with changes in global ocean chemistry, which is in turn believed to be tied to the production of the North Atlantic Bottom Water and/or ventilation via the Panama Seaway.

$\delta^{13}\text{C}$ data in the bulk-isotope record from Ocean Drilling Program Site 1256 show a close parallel with CaCO_3 mass accumulation rates (MARs) in the 5- to 14-Ma interval (correlation coefficient = 0.87), suggesting a relationship likely coupled to surface water productivity by calcite-secreting organisms. The decoupling between $\delta^{13}\text{C}$ and MARs after 5 Ma probably indicates a dominance of dissolution over carbonate production. Therefore, the coincidence in $\delta^{13}\text{C}$ excursions with the stages of sharp reduction in CaCO_3 MARs during the carbonate crash points to a causative mechanism induced by surface circulation-induced low productivity.

We speculate that the major middle/late Miocene sea level drop may have caused the complete closure of the Indonesian Seaway. We propose a model wherein the blockage of Indonesian Throughflow would have resulted in a piling-up of surface warm water in the west Pacific, thereby strengthening the Equatorial Undercurrent system. The eastward spread of this nutrient-poor water then warmed sea-surface temperature and reduced upwelling in the central and eastern Pacific, reducing in turn biological productivity of phytoplankton. A coincident reduction in Central America and circum-Caribbean volcanism

¹Jiang, S., Wise, S.W., Jr., and Wang, Y., 2007. Cause of the middle/late Miocene carbonate crash: dissolution or low productivity? *In* Teagle, D.A.H., Wilson, D.S., Acton, G.D., and Vanko, D.A. (Eds.), *Proc. ODP, Sci. Results*, 206: College Station, TX (Ocean Drilling Program), 1–24. doi:10.2973/odp.proc.sr.206.013.2007

²Department of Geological Sciences, 108 Carraway Building, Florida State University, Tallahassee FL 32306-4100, USA. Correspondence author: jiang@quartz.gly.fsu.edu

Initial receipt: 6 February 2006

Acceptance: 29 December 2006

Web publication: 30 April 2007

Ms 206SR-013

plus the deflection of the delivery of volcanic ash as a result of the then prevailing southeastern trade winds across the equator further deprived these regions of trace element nutrients, which added to lowered surface water carbonate production. Surface water warming and reduced upwelling is documented by negative excursions in $\delta^{18}\text{O}$ values. The reduction in carbonate supply to the deep waters caused a rapid shoaling of the carbonate compensation depth and triggered the carbonate crash. The close correlation between CaCO_3 mass accumulation rates and biological productivity suggests that the carbonate crash is best characterized as a low-productivity event.

INTRODUCTION

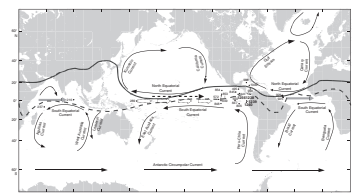
“Carbonate crash” is the term applied by Lyle et al. (1995) and Farrell et al. (1995) to a major middle/late Miocene carbonate shift in tropical regions characterized by a dramatic reduction of calcium carbonate content in sediments and poor preservation of calcareous microfossils. This phenomenon has been widely documented in the equatorial Pacific, Atlantic, and Indian Oceans (Lyle, 2003; King et al., 1997; Peterson et al., 1992; respectively), as well as in the Caribbean Sea (Roth et al., 2000), and provides a seismic reflector for long-range correlation (Mayer et al., 1986; Bloomer et al., 1995).

Several hypotheses have been advanced to account for the carbonate crash. Mechanisms recently proposed attributed it to enhanced dissolution (rather than reduced surface water productivity of calcite-secreting organisms) associated with changes in deepwater circulation and shoaling of the carbonate compensation depth (CCD) and/or lysocline (e.g., Farrell et al., 1995; Lyle et al., 1995; Roth et al., 2000). Alternatively, the crash may have resulted from a biologic bloom (Theyer et al., 1985) (i.e., decomposition of organic matter from increases in surface productivity can result in enhanced dissolution of carbonate through acid production where the ratio of organic carbon to carbonate is high in falling debris) (Emerson and Bender, 1981; Archer, 1991a, 1991b). Dilution by terrigenous or other noncarbonate sediments could also have caused carbonate reduction in the sediments (Keller and Barron, 1983; Diester-Haass et al., 2004). This scenario involves changes in sedimentation patterns probably driven by climate change and/or tectonic changes in basin configurations or closure of oceanographic pathways. A contemporary global sea level drop (Haq et al., 1987) was excluded because it is believed that the middle/late Miocene sea level drop is associated with a deepening of the CCD and enhanced carbonate preservation (Berger, 1970; Peterson et al., 1992).

The carbonate crash recorded in the Caribbean and major world oceans, however, seems to point to a common cause as indicated by the comparable nature and time overlap of its occurrences, a cause related to processes affecting the global carbonate and carbon budget. A determination of the role that carbonate dissolution, production, and dilution have played would help unravel the cause of the crash.

We present here an oxygen and carbon stable isotopic record and its correlation with carbonate mass accumulation rates (MARs) in sediments from Ocean Drilling Program (ODP) Site 1256 located in the eastern equatorial Pacific (Fig. F1). We then discuss the possible cause of the middle/late Miocene carbonate crash in light of these data.

F1. Site locations, p. 20.



BACKGROUND

Study Area

Site 1256 (6°44.2'N, 91°56.1'W) (Fig. F1), drilled during ODP Leg 206, lies in 3635 m water depth in the Guatemala Basin on Cocos plate crust that formed at ~15 Ma on the eastern flank of the East Pacific Rise (EPR) when the site experienced a superfast spreading rate (Wilson, 1996). This site formed at an equatorial latitude within the equatorial high-productivity zone and initially experienced very high sedimentation rates (39.1 m/m.y.) (e.g., Jiang and Wise, this volume). The high core recovery (89% with two-thirds of the cores taken by the advanced piston corer) and high sedimentation rates through critical time intervals provide an excellent opportunity for high-resolution paleoceanographic study.

The modern oceanographic setting in the equatorial world oceans is illustrated in Figure F1. This circulation pattern is a product of tropical atmospheric circulation and the Coriolis effect across the equator. Because the southeastern trade winds are stronger than the northeastern antithesis, they converge north of the equator to form the Intertropical Convergence Zone (ITCZ), a belt with weak winds and heavy rainfall forming a barrier for eolian dust between southern and northern sources (e.g., Rea, 1994; Pettke et al., 2002). As southeastern trade winds blow across the equator, the change in direction of the Coriolis effect causes divergence along the equator that results in a depression in surface topography and creates the pressure gradient that together produce a geostrophic flow (i.e., the South Equatorial Current [SEC]). In the Pacific, the waters flowing in the SEC originate from the Peru-Chile Current (PCC) and Equatorial Undercurrent (EUC) (Kessler, 2002, 2006). The strength of the SEC mimics the strength of the southeastern trade winds, whereas the North Equatorial Current and North Equatorial Countercurrent change intensity in response to the position of northeastern trade winds (Wyrтки, 1974).

The sediments of the eastern equatorial Pacific Ocean are known to be sensitive recorders of oceanographic changes and record a complex interplay of ocean chemistry, productivity, climate, and plate tectonics (e.g., van Andel et al., 1975). The high sedimentation rates are engendered by upwelling-driven, high biological productivity (e.g., van Andel et al., 1975; Murray et al., 1994; Lyle, 2003), which is estimated to contribute 18%–56% to the global new production (Chavez and Barber, 1987) (more recently revised to 26% [Chavez and Toggweiler, 1995]), although only corresponding to 3% of the global ocean area. This upwelling, resulting from the equatorial divergence under the influence of the Coriolis effect, provides major nutrients as well as elemental iron for phytoplankton (Landry et al., 1997), the primary producers in ocean surface waters and major contributors to deep-sea sediments. The bulk nutrients, however, are brought to the equator by the PCC with a shallow-water source (~50 m) (Wyrтки, 1981) of a subantarctic origin. Thus, the primary productivity in this region depends on the intensity of upwelling and the supply of nutrients imported at thermocline depths (e.g., Rea et al., 1991; Weber and Pisias, 1999). The latter, in turn, is controlled by the wind stress along the equator that affects the depth of the thermocline. Nutrients in this region, however, are not depleted by phytoplankton, a condition known as “high nutrient, low chlorophyll” (HNLC) (Minas et al., 1986), which is believed to be a result of iron limitation on large phytoplankton (Martin, 1990; Martin et

al., 1991; Barber and Chavez, 1991) and/or intense grazing control on small phytoplankton (Landry et al., 1997). Dissolved iron plays an essential role in controlling phytoplankton growth in the oceans (e.g., Weinberg, 1989; Coale et al., 1996; Hutchins and Bruland, 1998). This need for phytoplankton in open oceans can usually be met by the fall-out of Fe-rich eolian dust (including volcanic ash) (e.g., Martin and Gordon, 1988; Frogner et al., 2001), and/or by upwelling of deep water (e.g., Landry et al., 1997), although iron concentrations are very low due to its insolubility in oxygenated seawater, hence its fragile and transient bioavailability in the marine ecosystem.

Samples, Methods, and Age Constraints

Samples were taken aboard *JOIDES Resolution* at a spacing of two per section (~75 cm) for all cores from Hole 1256B. Stable oxygen and carbon isotopic analyses were carried out on each sample above 150.50 meters below seafloor. Below this depth, one sample per 4–10 m was selected for isotopic analysis to illustrate isotopic fluctuations prior to the carbonate crash.

Samples for oxygen and carbon isotope study were prepared on bulk sediments by grinding dried sediment to a homogeneous powder and baking at 425°C for 2 hr in vacuum. The stable carbon and oxygen isotopic ratios of the baked samples were analyzed using a Gas Bench II Auto-Carbonate device interfaced to a Finnigan MAT Delta plus XP mass spectrometer. All isotope results were calibrated against international and internal laboratory standards and expressed in standard delta notation relative to the Peedee belemnite standard. Analytical precision for isotope analyses was better than ±0.1‰. The carbonate concentration in each sample was derived by calibrating signal amplitude of the first CO₂ peak against those of carbonate standards, which are assumed to be pure carbonate. CaCO₃ MARs (in grams per square centimeter per thousand years) were calculated in using the following equation:

$$\text{CaCO}_3 \text{ MAR} = (\text{CaCO}_3 \% \times \text{bulk density} \times \text{linear sedimentation rate}).$$

The age model by **Jiang and Wise** (this volume) was followed in this study, which integrated paleomagnetic data from the upper 100 m and biostratigraphic datums from the entire sequence by best linear fit. Assuming a constant sedimentation rate, the age of an individual sample was obtained by extrapolating the sedimentation rate in the specific interval to the depth of this sample.

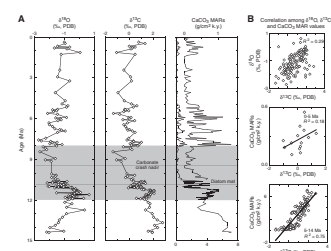
RESULTS

A bulk sediment stable isotope record spanning the entire sedimentary sequence is presented with CaCO₃ MARs in Figure F2A.

The oxygen isotope record shows marked variations from −2.7‰ to 0.6‰ (Fig. F2). The fluctuations of δ¹⁸O values show three major patterns:

1. An irregular but consistent long-term increase from −2.2‰ to 0.1‰ prior to 11.5 Ma,
2. A sudden decrease starting at ~11.5 Ma followed by two stepwise decreases reaching a nadir at ~10.0 Ma, and then

F2. MARs variations and correlations, p. 21.



- Swinging back and forth thereafter with a long-term increase.

Significant fluctuations are also present in the carbon isotope record, with a range from -1.4‰ to 2.8‰ (Fig. F2). $\delta^{13}\text{C}$ values are high and increase upsection just prior to 11.3 Ma, decrease sharply thereafter, recover somewhat from 11.1 to 11.7 Ma, decrease sharply again and remain low to the lowest point at ~ 8.5 Ma, and recover again thereafter. Two major negative excursions can be recognized at ~ 11.3 and ~ 10.7 Ma with a net reduction in $\delta^{13}\text{C}$ values over a range of $\sim 1.7\text{‰}$ and $\sim 1.6\text{‰}$, respectively. Carbon isotope values show little correlation with oxygen isotope records in the studied interval (Fig. F2B).

CaCO_3 MARs range from 0 to $7.06 \text{ g/cm}^2 \text{ k.y.}$ Variations in CaCO_3 MARs follow the trends in stable carbon isotopes prior to 5 Ma (correlation coefficient $[R] = 0.87$), but this positive correlation almost disappears thereafter ($R = 0.42$) (Fig. F2B).

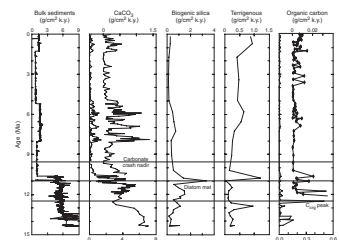
DISCUSSION

Bulk Carbonate Isotopes

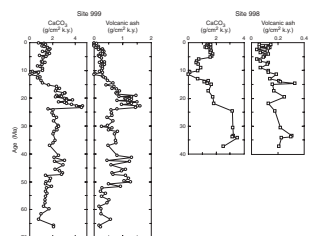
Stable oxygen and carbon isotopic measurements of single foraminiferal species have long been used in paleoceanographic and paleoclimatic studies because of the simpler interpretation of these data. In contrast, bulk carbonate isotopic ratios reflect weighted-average signals of different source materials, which complicates the interpretation and compromises the application of these data. Under certain circumstances, however, when the geological and sedimentary settings rule out enough such complications, bulk carbonate isotopic records can faithfully reproduce trends from a single foraminiferal species (Shackleton et al., 1993; Schrag et al., 1995); bulk carbonate has also been used for stable isotope analysis. Moreover, bulk isotopic analysis becomes the sole resort where the samples are too well lithified to allow separation of foraminifers, where foraminifers are sparse (which is the case here), and/or where very high sample resolution is desired over long intervals.

Site 1256 on the Cocos plate is separated from the west coast of Central America by the Middle American Trench, which traps most terrestrial sediments shed from the continent. The sedimentary sources, therefore, are mainly biogenic calcite and silica as indicated by the relationship of MARs between bulk sediments and the main sedimentary components (Fig. F3). These biogenic materials are produced almost entirely in surface waters, and the benthic component is minor (e.g., van Andel et al., 1975). Furthermore, smear slide examinations have shown that the sediments contain highly abundant calcareous nannofossils, abundant siliceous microfossils, and extremely rare foraminifers (Shipboard Scientific Party, 2003; Jiang and Wise, this volume). The survival and preservation of calcareous nannofossils are likely linked to fecal pellet transport through the water column, where organic coatings mitigate coccolith dissolution in the water column and at the seafloor (Honjo, 1976). Thus, calcareous nannofossils contributed the great majority of the carbonate and consequent stable isotopic signals. We recognize that bulk $\delta^{13}\text{C}$ can be affected by detrital input such as from volcanogenic sources; however, such inputs were negligible in our study area at the time of the carbonate crash, as indicated by the nearby Caribbean sites (Fig. F4).

F3. MARs relationships, p. 22.



F4. CaCO_3 and volcanic ash MARs, p. 23.



The influence of different vital effects of calcareous nannofossil species is expected to be minor. Stoll (2005) showed that nearly monogeneric nannofossil isotopic records closely parallel those from bulk carbonate, that the interspecific vital effect in nannofossil isotopic measurements is small, and that variable nannofossil assemblages do not significantly bias the isotopic records. Schrag et al. (1995) further demonstrated that bulk isotope data are less sensitive to compositional variations. In such a case where the nannofossil assemblage is dominated by reticulofenestrads before, during, and shortly after the carbonate crash (Jiang and Wise, this volume), bulk carbonate isotopes can be reliably used to investigate the cause of this event.

Carbonate Diagenesis

The dominant lithology in Hole 1256B is unconsolidated calcareous nannofossil ooze (Shipboard Scientific Party, 2003), consisting mainly of nannofossil skeletons of low-Mg calcium carbonate resistant to dissolution. Foraminifers are very rare and so are insufficient for isotopic analysis. Low-Mg carbonate is thermodynamically stable in deep, cold seawater and resistant to diagenetic alteration after deposition (Schlanger and Douglass, 1974); therefore, pelagic oozes remain virtually unlithified until buried to a certain depth, at which point CaCO_3 is released to the pore waters and reprecipitates as intraparticle fill, exterior overgrowth, and intergranular cement (Garrison, 1981).

Diagenetic alteration, including dissolution and postdepositional diagenesis, has potential for altering isotopic signals originally preserved in carbonates. Dissolution preferentially removes ^{13}C , resulting in a depletion of 0.2‰, as observed in benthic foraminifers (McCorkle et al., 1995), though theoretically higher depletion may occur under Rayleigh distillation. Burial diagenesis, increasing with increasing CaCO_3 content and burial depth, and diagenetic alteration by underlying basalts tend to progressively deplete heavier ^{18}O (Frank and Bernet, 2000; Schrag et al., 1992). Thus, severe diagenetic alteration produces isotopically lighter calcite with well-coupled stable oxygen and carbon values.

Carbon isotope data likely have been little affected by diagenetic alteration based on the following observations:

1. The calcareous nannofossil assemblage is moderately to well preserved (Jiang and Wise, this volume). This is especially true for the interval where the carbonate crash was documented.
2. The correlation coefficient is low between carbon and oxygen isotopes (Fig. F2B), which otherwise indicates precipitation of secondary isotopically lighter calcite cements attributed to an early diagenetic overprint (Jenkyns, 1974) or deep burial (Jenkyns and Clayton, 1986; Jenkyns, 1995).
3. An inverse relationship is absent between organic carbon and carbon isotope data (Figs. F2, F3) (Jenkyns and Clayton, 1986); therefore, carbon isotope values are considered to represent a primary environmental signal.

Oxygen isotope values are prone to diagenetic alteration during burial diagenesis because oxygen isotopes show significant temperature-dependent fractionation (Anderson and Arthur, 1983; Marshall, 1992). However, Schrag et al. (1995) demonstrated that the effect of rapid calcite precipitation is small for the biogenic carbonates from mid-latitude

Atlantic because primary oxygen isotope values in carbonates are close to isotopic equilibrium with cold pore fluids. As today, Site 1256 was located during the middle Miocene beneath the equatorial divergence and under a strong influence of upwelling of cold deep water, so the sea-surface temperatures (SSTs) are considered to be comparable to those of the temperate Atlantic as indicated by ocean SST pattern. The sediments at this site are shallowly buried (250.7 m), and hydrothermal circulation is no longer a major mechanism of heat transport (Shipboard Scientific Party, 2003). Therefore, oxygen isotope data mainly reflect environmental signals.

Carbonate Production Proxies

Paleoproductivity reconstruction is a major area of paleoceanographic research because it places important constraints on past ocean circulation, nutrient distribution, and oceanic carbon-cycle history. Important proxies have been developed for past productivity and interpreted in terms of organic carbon export. These proxies include direct measurements of organic carbon in sediments, biogenic opal and calcium carbonate accumulation, foraminiferal assemblage data, geochemical tracers, and $\delta^{13}\text{C}$ fluctuations (e.g., Müller and Suess, 1979; Berger et al., 1989; Herguera and Berger, 1991; Paytan et al., 1996; Tappan, 1968; respectively). In this study we employ CaCO_3 MARs and $\delta^{13}\text{C}$ values as proxies to assess changes in paleoproductivity (Fig. F3).

As the major components in the sediments are biogenic skeletons of organisms dwelling in the uppermost water column (Fig. F3), the geochemical composition of the sediments predominantly reflects a surface water signal. Thus, CaCO_3 MARs reflect carbonate production by surface-dwelling, calcite-secreting organisms when dissolution is a minor effect.

Interpretation of $\delta^{13}\text{C}$, however, depends on the specific geological and oceanographic setting. The bulk carbonate in this study was produced nearly exclusively in the surface water; therefore, variations in the bulk $\delta^{13}\text{C}$ values should reflect fluctuations therein, which are the product of the interplay between phytoplankton photosynthesis and surface water chemistry as influenced by seawater alkalinity and the dissolved carbon $^{13}\text{C}/^{12}\text{C}$ ratio. Phytoplankton dwell in the oceanic euphotic layer and preferentially take up ^{12}C during photosynthesis, producing organic matter with $\delta^{13}\text{C}$ values from -20‰ to $\sim 23\text{‰}$ and a relatively ^{13}C enriched, dissolved inorganic carbon pool in surface waters. Seawater pH influences the concentrations of different forms of dissolved inorganic carbon, the $\delta^{13}\text{C}$ values of which decrease with increasing seawater CO_3^{2-} (Spero et al., 1997).

In the present study, the close coupling between the CaCO_3 MARs and $\delta^{13}\text{C}$ values prior to 5 Ma and decoupling thereafter (Fig. F2B) reflect a switch of dominance between carbonate production and dissolution. Prior to 5 Ma, carbonate production controlled the sedimentary patterns at Site 1256 and $\delta^{13}\text{C}$ variations predominantly reflected changes in the standing stock of carbonate-producing organisms in the surface waters (Figs. F2, F3). After 5 Ma, dissolution dominated this site, probably resulting from the effective blocking of the Panama Seaway since then (Haug and Tiedemann, 1998).

The large excursions observed in $\delta^{13}\text{C}$ values could not have arisen from enhanced dissolution. Dissolution occurs when there is a reduction in CO_3^{2-} in the surface water, the water column that the carbonates

travel through, and the bottom water. Changes in seawater CO_3^{2-} in intermediate and deep waters, however, do not significantly alter the $\delta^{13}\text{C}$ signal of carbonates produced, as observed in foraminifers (McCorkle et al., 1995). If such reduction in CO_3^{2-} occurred in surface waters, it would have greatly increased the $\delta^{13}\text{C}$ and $\delta^{18}\text{O}$ values of carbonate (Spero et al., 1997), a situation that is opposite from the observations here (Fig. F2). Therefore, no matter where severe dissolution occurs, it could not produce the negative excursions in $\delta^{13}\text{C}$ and $\delta^{18}\text{O}$ values observed in this study. $\delta^{13}\text{C}$ values faithfully represent variations in the surface water standing stock of calcite producers.

Carbonate Crash

Timing of Carbonate Crash

CaCO_3 sedimentation at Site 1256 shows several extreme lows between 12 and 8 Ma, which were initiated at ~11.3 and 10.6 Ma, geologically synchronous with the onset of the carbon isotope excursions (Fig. F2). The deepest drop is at 9.6 Ma, with carbonate accumulation virtually ceasing. This is temporally comparable with the “nadir” of the carbonate crash at other ODP/Deep Sea Drilling Project (DSDP) sites in this region (Lyle et al., 1995; Farrell et al., 1995), whereas the five carbonate minima in the Caribbean occurred ~1 m.y. earlier (12–10 Ma) (Roth et al., 2000). These phenomena were previously ascribed to enhanced carbonate dissolution as a consequence of changes in deepwater circulation (e.g., Lyle et al., 1995; Roth et al., 2000).

Carbonate Accumulation in Open Oceans

On the ocean floor, dissolution of calcium carbonate in seawater is determined by seawater pH values influenced by temperature, pressure, and the partial pressure of CO_2 . The depth of the CCD varies in different ocean basins depending on bottom water chemistry and carbonate supply from surface water (Wise, 2003). The former explains a present-day CCD in the Pacific shallower than in the Atlantic, the latter a shallower CCD in high latitudes where carbonate production is low. High biological productivity tends to stimulate higher rates of carbonate production and to depress the CCD. However, if high productivity is engendered by extremely high concentrations of nutrients, a condition that favors diatoms and dinoflagellates, the CCD tends to shoal as a result of addition of CO_2 to the bottom water and/or acid production resulting from the degradation of organic matter (Emerson and Bender, 1981; Archer, 1991a, 1991b). This scenario may occur in response to changes in climate (Dymond and Lyle, 1985).

Previous Models for the Carbonate Crash

Multiple causative mechanisms have been proposed for the carbonate crash. Severe dissolution in the equatorial Pacific and Caribbean has been attributed to changes in bottom water chemistry. The underlying hypotheses are either

1. The early phase of constriction of the Panama Seaway that restricted the exchange of high- CO_3^{2-} deep waters between the Pacific and the Caribbean (Lyle et al., 1995; Farrell et al., 1995) or

2. The intensified influx of corrosive water in response to strengthened global thermohaline circulation linked to enhanced production of North Atlantic Deep Water (NADW) (Roth et al., 2000).

Although the “nadir” of the carbonate crash occurred ~1 m.y. earlier in the Caribbean than elsewhere, the comparable nature and time overlap of its occurrences suggest a common cause associated with changing oceanic circulation (Roth et al., 2000). This does not exclude other competitive mechanisms, such as “dilution” by terrigenous sediments (Diester-Haass et al., 2004) or an opal component (Westerhold et al., 2003; Böhm and Dullo, 2000) for those “carbonate crashes” reported elsewhere (i.e., the southern and eastern South Atlantic, southern Indian Ocean).

Phytoplankton community restructuring against calcite-producing organisms could also produce severe reduction in CaCO_3 MARs, even though the overall surface water productivity remains constant (Dymond and Lyle, 1985). At Site 1256, the negative excursions in $\delta^{13}\text{C}$ and $\delta^{18}\text{O}$ coincide prior to the carbonate crash. At this time, an oxygen isotope signal is supposed to record a combination of surface temperature, ice volume, and seawater chemistry, the latter two of which tend to enrich heavier isotopes in response to the development of the East Antarctic Ice Sheet (EAIS) (Zachos et al., 2001) and, if any, the dissolution-related decrease in seawater CO_3^{2-} . Thus, $\delta^{13}\text{C}$ excursions observed at Site 1256 likely represent sudden SST increases, a condition that favors warm-water specialists/calcite-producing organisms (McIntyre and Bé, 1967; McIntyre et al., 1970). Similar observations, especially the coeval excursion in $\delta^{13}\text{C}$ and $\delta^{18}\text{O}$ values at 11.3 Ma, have also been documented in other nearby ODP/DSDP sites (Shackleton and Hall, 1984, 1995) and in the Caribbean (Mutti, 2000). In other words, these $\delta^{13}\text{C}$ excursions represent a sharp decrease in standing stock of calcareous phytoplankton in surface waters.

Evidence for increased dissolution across the carbonate crash includes a decreased coarse calcareous fraction, increased benthic/planktonic foraminifer ratios, and deteriorated preservation of calcareous fossils. These indirect proxies should be cautiously placed into a sedimentary and geochemical context. The drop in the sand-sized fraction recorded at Sites 998 and 999 was attributed to enhanced fragmentation of foraminiferal tests in more corrosive water columns (Roth et al., 2000), whereas the same phenomenon observed in the southeast Atlantic (Sites 1085 and 1087) was related to sea level regression and consequent increased terrestrial input (Diester-Haass et al., 2004). The increased corrosiveness of the water column itself, however, does not necessarily demand an influx of corrosive waters because a reduction in carbonate production in the surface water would have the same effect. The increase in the ratios of benthic to planktonic foraminifers in the southwest Atlantic seems to be controlled more by nutrient condition than dissolution (Diester-Haass et al., 2004). At Site 1256, the calcareous nannofossil assemblages exhibit their best preservation just prior to the carbonate crash nadir (Jiang and Wise, this volume). This does not necessarily mean no dissolution occurred during the two dramatic drops in carbonate MARs because the preservation is closely associated with the presence and abundance of diatoms, which release silica to pore waters and thus inhibit dissolution and/or precipitation of calcite during diagenesis (Wise, 1977).

Constriction of the Panama Seaway in the late middle Miocene limited communication between the Atlantic and Pacific at intermediate and deep-water levels (Duque-Caro, 1990) and could have caused basin-to-basin isotopic fractionation (Lyle et al., 1995; Roth et al., 2000), a scenario seen today. The modern Atlantic is filled with young, well-oxygenated water as a result of the production of NADW, whereas the Pacific has older water originating from the North Atlantic and southern high latitudes. As these waters age, the organic matter therein decomposes and releases ^{12}C -depleted carbon into seawater, which is responsible for the more negative $\delta^{13}\text{C}$ values in eastern Pacific relative to the western Atlantic (Fig. F5) (Kroopnick, 1985). However, the following perceptions raise several questions regarding this mechanism.

It takes ~1500 yr for deep water sinking in the North Atlantic to reach the North Pacific (Manighetti, 2001), which cannot explain the 1-m.y. lead for the carbonate crash in the Caribbean. The water brought up to the surface by equatorial divergence-driven upwelling has a shallow-water source above the thermocline with a mean depth of 50 m (Vossepoel et al., 1999). In fact, no matter where the ultimate source of these waters is, the North Atlantic or circumpolar Antarctic, the $\delta^{13}\text{C}$ difference between these sources today and the eastern Pacific is no more than 0.7‰ (Fig. F5). This alone could not have caused the $\delta^{13}\text{C}$ excursions of >1.6‰ accompanying the carbonate crash documented at Site 1256. The carbonate crash was observed mostly from records retrieved from >3000 m water depth, a depth level that is highly sensitive to fluctuations in the CCD in the eastern equatorial basins (Lyle et al., 1995). The previously proposed mechanisms can hardly account for its occurrences at very shallow sites (e.g., Sites 1000 and 1241) in water depths well above the modern CCD, hence, the least susceptible to the influence of shoaling CCDs.

As a matter of fact, carbonate production played a dominant role over dissolution as evidenced by the close parallelism in CaCO_3 MARS and $\delta^{13}\text{C}$ values in the 14- to 5-Ma interval and by the absence of deterioration in preservation of calcareous nannofossils during the crash (Raffi and Flores, 1995; Jiang and Wise, this volume). In other words, the crash was not a dissolution event but a low-productivity event. This conclusion is in line with the lack of basinwide occurrences of the crash in the Pacific (Lyle, 2003).

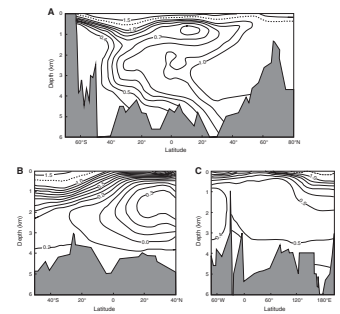
Proposed Model for the Carbonate Crash

Based on these observations and discussions above, we speculate that a reduction in the standing stock of carbonate-producing organisms, likely induced by a reduction in nutrient availability, triggered the widespread carbonate crash at the middle/late Miocene boundary.

The model proposed here emphasizes that carbonate supply to intermediate and deep waters is primarily a function of changes in carbonate production and, as a consequence, affects the corrosiveness of these waters on carbonate and preservation of carbonate. The change of carbonate production is associated with changing global surface water circulation, which, in turn, is induced by the seaway-controlled interocean exchange of water masses.

During the late Cenozoic, prior to the segmentation of the once virtually continuous circumequatorial current, nutrient-rich intermediate water was tapped out to the surface, where it sustained high biological productivity along the equator. This flow began to fragment because of the uplift of the Panama Isthmus at 12.9–11.8 Ma (Duque-Caro, 1990)

F5. Atlantic, Pacific, and Antarctic $\delta^{13}\text{C}$, p. 24.



and the closure of the Indonesian Seaway at 12–11 Ma (Keller, 1985; Romine and Lombardi, 1985; Kennett et al., 1985). The latter occurred when subduction developed on the east and west sides of New Guinea (Hall, 2001). The difference in timing can explain the ~1-m.y. lead of the carbonate crash in the Caribbean relative to the Pacific and Indian Oceans.

Although the Indonesian Seaway was effectively blocked at ~17–15 Ma, Indo-Pacific communication was still possible through small passages during times of high sea level (Nishimura and Suparka, 1997). This transport of surface water, termed the Indonesian Throughflow (ITF) today, carries warm and fresh tropical-Pacific surface water through this passage into the Indian Ocean and creates a warm pool in the western Indian Ocean. Global sea level drop at the middle/late Miocene boundary (Haq et al., 1987; Sen et al., 1999) may have completely blocked this Pacific-to-Indian surface water transport, switching the locale for warm water accumulation to the western Pacific, creating a greater warm pool there. The eastward spread of the warm-pool water strengthened the EUC system (Kennett et al., 1985), resulting in warm SSTs in the central and eastern Pacific and reduced equatorial upwelling of colder subsurface water, both of which contribute to the creation of a $\delta^{18}\text{O}$ excursion. The switch of dominance to nutrient-poor warm surface water caused a sudden reduction in biological productivity, which is represented by a $\delta^{13}\text{C}$ excursion. This event is analogous to today's El Niño. A similar scenario may have occurred in the Caribbean and Atlantic when the Panama Seaway suddenly became restricted at 12.9–11.8 Ma.

Because blockage of the ITF cut off Pacific-to-Indian Ocean heat transport, this should have triggered an overall warming in the tropical Pacific and cooling in the southern Indian Ocean. This is evidenced by an abrupt disappearance of foraminiferal and radiolarian provincialism across the equatorial Pacific (Keller, 1985; Romine and Lombardi, 1985; Kennett et al., 1985) and a positive $\delta^{18}\text{O}$ excursion in shallow-dwelling planktonic foraminifers at DSDP Sites 216 and 237 (Vincent et al., 1985). A temporally similar warming of the entire water column was recorded at DSDP Site 289 (Gasperi and Kennett, 1993). The eastern spread of warm surface water warmed not only the east equatorial Pacific, but also the southeast Pacific off Chile (Tsuchi, 1997). These perceptions are consistent with the results of a near-global ocean general circulation model for the circulation and thermal structure of the Pacific and Indian Oceans with open and closed Indonesian passages from 1981 to 1997 proposed by Lee et al. (2002).

It is worth mentioning that the evolution of global climate entered a full ice-house mode during the Neogene (Zachos et al., 2001). Cold climate narrows carbonate producing areas, rendering carbonate production in tropical oceans more important; small changes in production therein greatly affect total carbonate supply to deep waters. After full development of the EAIS by the middle Miocene (Shackleton and Kennett, 1975; Kennett et al., 1985; Woodruff and Savin, 1991; Zachos et al., 2001) (North Hemisphere glaciations did not begin until ~7 Ma [Fronval and Jansen, 1996]), the southern trade winds began to prevail over their northern counterpart, causing a northward shift of the ITCZ, an analog of the initiation of modern North Hemisphere summers. The intensification of southeastern trade winds during the Neogene is consistent with the coarsening of eolian grain size recorded from the subtropical South Pacific (Rea and Bloomstine, 1986). Positions farther north than present (5°N) of $10^\circ\text{--}12^\circ\text{N}$, $\sim 22^\circ\text{--}24^\circ\text{N}$, and $13^\circ\text{--}14^\circ\text{N}$ have been suggested for the ITCZ around the middle/late Miocene boundary

by Flöhn (1981), Rea (1994), and Shipboard Scientific Party (2002), respectively. This northward shift of the ITCZ can potentially wash out eolian dust at the northern mid-latitudes, mitigating the iron-limited condition and stimulating biological production. This scenario is consistent with the records from North Pacific (Snoeckx et al., 1995).

The eastern equatorial Pacific is presently an HNLC region because of iron limitation on phytoplankton (Martin et al., 1991). This region did not suffer from iron deficiency during the early and middle Miocene when there was intense activity in circum-Caribbean and Central American volcanism as evidenced by tephra accumulation rates (Sigurdsson et al., 2000), but it has since then. Once exposed to seawater, volcanic ash can fertilize the open ocean by releasing large amounts of macronutrients and bioactive trace metals (Frogner et al., 2001).

According to our model, with the closure of the Indonesian Seaway by sea level drop at the middle/late Miocene boundary, warm surface water began to pile up in the western Pacific. The formation of a larger warm pool strengthened the EUC system. The eastward spread of this water triggered a prominent El Niño, reducing upwelling and then nutrient availability. At the same time, prevailing southeastern trade winds across the equator deflected the delivery of volcanic ash from Central America and the circum-Caribbean, where coincidentally volcanism was reduced sharply (Sigurdsson et al., 2000). The decrease in availability of macronutrients and micronutrients resulted in a drastic reduction in primary productivity in the eastern and central equatorial Pacific as well as the Caribbean, as evidenced by the carbon isotope excursions at Site 1256 and the synchronous variations in MARs of carbonate and volcanic ash throughout the Neogene at Sites 998 and 999 (Fig. F4).

The CCD in the Neogene Pacific is a product of the balance between regional production and basinwide dissolution (Lyle, 2003). The modern deep Pacific below 1500 m is essentially a single water mass (Joyce et al., 1986; Talley and Roemmich, 1991); therefore, the entire Pacific Ocean floor is bathed by the same water mass and carbonate dissolves primarily at the ocean floor (Edmond, 1974; Walsh et al., 1988). On one hand, dissolution rates should be similar everywhere and there should be a base-level CCD for all regions in the Pacific. The variable depth of the CCD in the Pacific, however, originates from biogeographic differences (Lyle, 2003). That is, although there is a base level, the CCD may be depressed or elevated depending on surface productivity. On the other hand, although there has always been during the Neogene an Antarctic deepwater source into the Pacific Basin, no convincing evidence exists for stronger flow at the middle/late Miocene boundary (Lyle et al., 1995). The consequent near-constant deepwater chemistry, plus the close correlation between CaCO_3 MARs and biological productivity, suggest that the carbonate crash in the eastern equatorial Pacific and likely in other regions is not a dissolution event, but one of low productivity.

CONCLUSIONS

The late/middle Miocene carbonate crash has previously been considered only a dissolution event associated with production of North Atlantic Bottom Water and ventilation via the Panama Seaway. A coupling between $\delta^{13}\text{C}$ and CaCO_3 MARs data in the 5- to 14-Ma interval ($R = 0.87$) observed at ODP Site 1256 suggests a dominant role for car-

bonate production by calcite-secreting organisms in surface waters, whereas the decoupling thereafter probably indicates enhanced dissolution caused by the effective closure of the Panama Seaway. Therefore, the coeval occurrences of negative $\delta^{13}\text{C}$ excursions and stages of sharp reduction in CaCO_3 MARs during the middle/late Miocene carbonate crash point to a causative mechanism related to surface circulation-induced low fertility.

We speculate that the major middle/late Miocene sea level drop caused complete closure of the Indonesian Seaway. Blockage of the ITF resulted in a piling-up of surface warm water in the west Pacific, strengthening the EUC system. We further speculate that the eastward spread of this nutrient-poor water warmed the SST and reduced upwelling in the central and eastern Pacific, primarily triggering a reduction in the standing stock in calcareous phytoplankton. The synchronous reduction in Central America and circum-Caribbean volcanism and deflected delivery of volcanic ash would have further deprived these regions of trace elements, which added to lowered surface water carbonate production. Surface water warming and reduced upwelling is documented by a negative excursion in $\delta^{18}\text{O}$ values. The reduction in carbonate supply to the deep waters caused a rapid shoaling of the CCD and triggered the carbonate crash. The close coupling between CaCO_3 MARs and biological productivity suggests that the carbonate crash is not a dissolution event but one caused by a marked drop in productivity.

Further work to test the mechanism proposed here is needed to compare the variations at the sea surface, thermocline, and, if possible, seafloor. This should be possible by comparing paleothermal records (e.g., $\delta^{18}\text{O}$, Mg/Ca ratios, Sr/Ca ratios, U^{k}_{37} index, etc.) spanning the carbonate crash from shallower localities in the east and west Pacific, respectively, where foraminifers are well preserved. To simplify the interpretation of the isotopic data, it would be ideal to analyze a single foraminiferal species from niches at different water depths.

ACKNOWLEDGMENTS

We wish to thank all the participants of ODP Leg 206 for their contributions relevant to this paper and Dana Biasatti from the Stable Isotope Laboratory in National High Magnetic Field Laboratory for her helpful assistance in running samples. The concept of this paper has been presented in abstract by Jiang et al. (2006). We thank Drs. Gerald J. Dickens, Mitchell W. Lyle, Larry C. Peterson, Gary Acton, and an anonymous reviewer for helpful and constructive reviews. This research used samples and/or data provided by the Ocean Drilling Program (ODP). ODP is sponsored by the U.S. National Science Foundation (NSF) and participating countries under management of Joint Oceanographic Institutions (JOI), Inc. Funding for this research was provided by a United States Science Advisory Committee grant to S.J. and S.W.W. (Task Order F001790). General laboratory support was provided by NSF-OPP 0126218 to S.W.W.

REFERENCES

- Anderson, T.F., and Arthur, M.A., 1983. Stable isotopes of oxygen and carbon and their applications to sedimentologic and paleoenvironmental problems. In Arthur, M.A., Anderson, T.F., Kaplan, I.F., Veizer, J., and Land, L.S. (Eds.), *Stable Isotopes in Sedimentary Geology*. SEPM Short Course, 10.
- Archer, D., 1991a. Modeling the calcite lysocline. *J. Geophys. Res., [Oceans]*, 96(9):17037–17050.
- Archer, D.E., 1991b. Equatorial Pacific calcite preservation cycles: production or dissolution? *Paleoceanography*, 6(5):561–571.
- Barber, R.T., and Chavez, F.P., 1991. Regulation of primary productivity rate in the equatorial Pacific Ocean. *Limnol. Oceanogr.*, 36:1803–1815.
- Berger, W.H., 1970. Biogenous deep-sea sediments: fractionation by deep-sea circulation. *Geol. Soc. Am. Bull.*, 81:1385–1401.
- Berger, W.H., Smetacek, V.S., and Wefer, G., 1989. Ocean productivity and paleoproductivity: an overview. In Berger, W.H., Smetacek, V.S., and Wefer, G. (Eds.), *Productivity of the Oceans: Present and Past*: New York (Wiley and Sons), 1–34.
- Bloomer, S.F., Mayer, L.A., and Moore, T.C., Jr., 1995. Seismic stratigraphy of the eastern equatorial Pacific Ocean: paleoceanographic implications. In Pisias, N.G., Mayer, L.A., Janecek, T.R., Palmer-Julson, A., and van Andel, T.H. (Eds.), *Proc. ODP, Sci. Results*, 138: College Station, TX (Ocean Drilling Program), 537–553. [doi:10.2973/odp.proc.sr.138.128.1995](https://doi.org/10.2973/odp.proc.sr.138.128.1995)
- Böhm, F., and Dullo, W., 2000. Neogene sedimentation at the central Kerguelen Plateau: coccoliths, diatoms, pumice and a “carbonate crash.” *Eos, Trans. Am. Geophys. Union*, 81(Suppl.):V41A-13. (Abstract)
- Chavez, F.P., and Barber, R.T., 1987. An estimate of new production in the equatorial Pacific. *Deep-Sea Res., Part A*, 34(7):1229–1243. [doi:10.1016/0198-0149\(87\)90073-2](https://doi.org/10.1016/0198-0149(87)90073-2)
- Chavez, F.P., and Toggweiler, J.R., 1995. Physical estimates of global new production: the upwelling contribution. In Summerhayes, C.P., Emeis, K.-C., Angel, M.V., Smith, R.L., and Zeitzschel, B. (Eds.), *Upwelling in the Ocean: Modern Processes and Ancient Records*: New York (Wiley), 313–320.
- Coale, K.H., Johnson, K.S., Fitzwater, S.E., Gordon, R.M., Tanner, S., Chavez, F.P., Ferioli, L., Sakamoto, C., Rogers, P., Millero, F., Steinberg, P., Nightingale, P., Cooper, D., Cochlan, W.P., Landry, M.R., Constantinou, J., Rollwagen, G., Trasvina, A., and Kudela, R., 1996. A massive phytoplankton bloom induced by an ecosystem-scale iron fertilization experiment in the equatorial Pacific Ocean. *Nature (London, U. K.)*, 383(6600):495–501. [doi:10.1038/383495a0](https://doi.org/10.1038/383495a0)
- Diester-Haass, L., Meyers, P.A., and Bickert, T., 2004. Carbonate crash and biogenic bloom in the late Miocene: evidence from ODP Sites 1085, 1086, and 1087 in the Cape Basin, southeast Atlantic Ocean. *Paleoceanography*, 19(1):PA1007. [doi:10.1029/2003PA000933](https://doi.org/10.1029/2003PA000933)
- Duque-Caro, H., 1990. Neogene stratigraphy, paleoceanography and paleobiogeography in northwest South America and the evolution of the Panama Seaway. *Palaeogeogr., Palaeoclimatol., Palaeoecol.*, 77(3–4):203–234. [doi:10.1016/0031-0182\(90\)90178-A](https://doi.org/10.1016/0031-0182(90)90178-A)
- Dymond, J., and Lyle, M., 1985. Flux comparisons between sediments and sediment traps in the eastern tropical Pacific: implications for atmospheric CO₂ variations during the Pleistocene. *Limnol. Oceanogr.*, 30:699–712.
- Edmond, J.M., 1974. On the dissolution of carbonate and silicate in the deep ocean. *Deep-Sea Res.*, 21:455–480.
- Emerson, S., and Bender, M., 1981. Carbon fluxes at the sediment-water interface of the deep-sea: calcium carbonate preservation. *J. Mar. Res.*, 39:139–162.
- Farrell, J.W., Raffi, I., Janecek, T.R., Murray, D.W., Levitan, M., Dadey, K.A., Emeis, K.-C., Lyle, M., Flores, J.-A., and Hovan, S., 1995. Late Neogene sedimentation patterns in the eastern equatorial Pacific Ocean. In Pisias, N.G., Mayer, L.A., Janecek, T.R., Palmer-Julson, A., and van Andel, T.H. (Eds.), *Proc. ODP, Sci. Results*,

- 138: College Station, TX (Ocean Drilling Program), 717–756. doi:10.2973/odp.proc.sr.138.143.1995
- Flöhn, H., 1981. A hemispheric circulation asymmetry during late Tertiary. *Geol. Rundsch.*, 70(2):725–736. doi:10.1007/BF01822146
- Frank, T.D., and Bernet, K., 2000. Isotopic signature of burial diagenesis and primary lithological contrasts in periplatform carbonates (Miocene, Great Bahama Bank). *Sedimentology*, 47(6):1119–1134. doi:10.1046/j.1365-3091.2000.00344.x
- Frogner, P., Gíslason, S.R., and Óskarsson, N., 2001. Fertilizing potential of volcanic ash in ocean surface water. *Geology*, 29(6):487–490. doi:10.1130/0091-7613(2001)029<0487:FPOVAI>2.0.CO;2
- Fronval, T., and Jansen, E., 1996. Late Neogene paleoclimates and paleoceanography in the Iceland-Norwegian Sea: evidence from the Iceland and Vøring Plateaus. In Thiede, J., Myhre, A.M., Firth, J.V., Johnson, G.L., and Ruddiman, W.F. (Eds.), *Proc. ODP, Sci. Results*, 151: College Station, TX (Ocean Drilling Program), 455–468. doi:10.2973/odp.proc.sr.151.134.1996
- Garrison, R.E., 1981. Diagenesis of ocean carbonate sediments: a review of the DSDP perspective. In Warme, J.E., Douglas, R.G., and Winterer, E.L. (Eds.), *The Deep Sea Drilling Project: A Decade of Progress*. Spec. Publ.—Soc. Econ. Paleontol. Mineral., 32:181–207.
- Gasperi, J.T., and Kennett, J.P., 1993. Vertical thermal structure evolution of Miocene surface waters: western equatorial Pacific DSDP Site 289. *Mar. Micropaleontol.*, 22(3):235–254. doi:10.1016/0377-8398(93)90046-Z
- Hall, R., 2001. Extension during late Neogene collision in east Indonesia and New Guinea. In Ailleres, L., and Rawling, T. (Eds.), *Animations in Geology*. J. Virtual Explor., 4:17–24.
- Haq, B.U., Hardenbol, J., and Vail, P.R., 1987. Chronology of fluctuating sea levels since the Triassic. *Science*, 235(4793):1156–1167. doi:10.1126/science.235.4793.1156
- Haug, G.H., and Tiedemann, R., 1998. Effect of the formation of the Isthmus of Panama on Atlantic Ocean thermohaline circulation. *Nature (London, U. K.)*, 393(6686):673–676. doi:10.1038/31447
- Herguera, J.C., and Berger, W.H., 1991. Paleoproductivity from benthic foraminifera abundance: glacial to postglacial change in the west-equatorial Pacific. *Geology*, 19(12):1173–1176. doi:10.1130/0091-7613(1991)019<1173:PFBFAG>2.3.CO;2
- Honjo, S., 1976. Coccoliths: production, transportation and sedimentation. *Mar. Micropaleontol.*, 1:65–79. doi:10.1016/0377-8398(76)90005-0
- Hutchins, D.A., and Bruland, K.W., 1998. Iron-limited diatom growth and Si:N uptake ratios in a coastal upwelling regime. *Nature (London, U. K.)*, 393(6685):561–564. doi:10.1038/31203
- Jenkyns, H.C., 1974. Origin of red nodular limestones (Ammonitico Rosso, Knollenkalke) in the Mediterranean Jurassic: a diagenetic model. In Hsü, K.J., and Jenkyns, H.C. (Eds.), *Pelagic Sediments: On Land and Under the Sea*. Spec. Publ. Int. Assoc. Sedimentol., 1:249–271.
- Jenkyns, H.C., 1995. Carbon-isotope stratigraphy and paleoceanographic significance of the Lower Cretaceous shallow-water carbonates of Resolution Guyot, Mid-Pacific Mountains. In Winterer, E.L., Sager, W.W., Firth, J.V., and Sinton, J.M. (Eds.), *Proc. ODP, Sci. Results*, 143: College Station, TX (Ocean Drilling Program), 99–104. doi:10.2973/odp.proc.sr.143.213.1955
- Jenkyns, H.C., and Clayton, C.J., 1986. Black shales and carbon isotopes in pelagic sediments from the Tethyan Lower Jurassic. *Sedimentology*, 33(1):87–106. doi:10.1111/j.1365-3091.1986.tb00746.x
- Jiang, S., Wise, S.W., and Wang, Y., 2006. Persistent El Niño-like conditions during the middle/late Miocene carbonate crash. *Eos, Trans. Am. Geophys. Union*, 87(36)(Suppl.):V44B-03. (Abstract)
- Joyce, T.M., Warren, B.A., and Talley, L.D., 1986. The geothermal heating of the abyssal subarctic Pacific Ocean. *Deep-Sea Res., Part A*, 33(8):1003–1015. doi:10.1016/0198-0149(86)90026-9

- Keller, G., 1985. Depth stratification of planktonic foraminifers in the Miocene ocean. In Kennett, J.P. (Ed.), *The Miocene Ocean: Paleoceanography and Biogeography*. Mem.—Geol. Soc. Am., 163:177–196.
- Keller, G., and Barron, J.A., 1983. Paleoceanographic implications of Miocene deep-sea hiatuses. *Geol. Soc. Am. Bull.*, 97:590–613.
- Kennett, J.P., Keller, G., and Srinivasan, M.S., 1985. Miocene planktonic foraminiferal biogeography and paleoceanographic development of the Indo-Pacific region. In Kennett, J.P. (Ed.), *The Miocene Ocean: Paleoceanography and Biogeography*. Mem.—Geol. Soc. Am., 163:197–236.
- Kessler, W.S., 2002. Mean three-dimensional circulation in the northeast tropical Pacific. *J. Phys. Oceanogr.*, 32:2457–2471.
- Kessler, W.S., 2006. The circulation of the eastern tropical Pacific: a review. *Progr. Oceanogr.*, 69(2–4):181–217. doi:10.1016/j.pocean.2006.03.009
- King, T.A., Ellis, W.G., Jr., Murray, D.W., Shackleton, N.J., and Harris, S., 1997. Miocene evolution of carbonate sedimentation at the Ceara Rise: a multivariate data/proxy approach. In Shackleton, N.J., Curry, W.B., Richter, C., and Bralower, T.J. (Eds.), *Proc. ODP, Sci. Results*, 154: College Station, TX (Ocean Drilling Program), 349–365. doi:10.2973/odp.proc.sr.154.116.1997
- Kroopnick, P.M., 1985. The distribution of ^{13}C of ΣCO_2 in the world oceans. *Deep-Sea Res., Part A*, 32(1):57–84. doi:10.1016/0198-0149(85)90017-2
- Landry, M.R., Barber, R.T., Bidigare, R.R., Chai, F., Coale, K.H., Dam, H.G., Lewis, M.R., Lindley, S.T., McCarthy, J.J., Roman, M.R., Stoecker, D.K., Verity, P.G., and White, J.R., 1997. Iron and grazing constraints on primary production in the central equatorial Pacific: an EqPac synthesis. *Limnol. Oceanogr.*, 42:405–418.
- Lee, T., Fukumori, I., Menemenlis, D., Xing, Z., and Fu, L.-L., 2002. Effects of the Indonesian Throughflow on the Pacific and Indian Oceans. *J. Phys. Oceanogr.*, 32(5):1404–1429. doi:10.1175/1520-0485(2002)032<1404:EOTITO>2.0.CO;2
- Lyle, M., 2003. Neogene carbonate burial in the Pacific Ocean. *Paleoceanography*, 18(3):1059. doi:10.1029/2002PA000777
- Lyle, M., Dadey, K.A., and Farrell, J.W., 1995. The late Miocene (11–8 Ma) eastern Pacific carbonate crash: evidence for reorganization of deep-water circulation by the closure of the Panama Gateway. In Piasias, N.G., Mayer, L.A., Janecek, T.R., Palmer-Julson, A., and van Andel, T.H. (Eds.), *Proc. ODP, Sci. Results*, 138: College Station, TX (Ocean Drilling Program), 821–838. doi:10.2973/odp.proc.sr.138.157.1995
- Manighetti, B., 2001. Ocean circulation: the planet's great heat engine. *Water Atmos.*, 9(4):12–14.
- Marshall, J.D., 1992. Climatic and oceanographic signals from the carbonate rock record and their preservation. *Geol. Mag.*, 129:143–160.
- Martin, J.H., 1990. Glacial–interglacial CO_2 change: the iron hypothesis. *Paleoceanography*, 5:1–13.
- Martin, J.H., and Gordon, R.M., 1988. Northeast Pacific iron distributions in relation to phytoplankton productivity. *Deep-Sea Res., Part A*, 35(2):177–196. doi:10.1016/0198-0149(88)90035-0
- Martin, J.H., Gordon, R.M., and Fitzwater, S.E., 1991. The case for iron. *Limnol. Oceanogr.*, 36:1793–1802.
- Mayer, L.A., Shipley, T.H., and Winterer, E.L., 1986. Equatorial Pacific seismic reflectors as indicators of global oceanographic events. *Science*, 233(4765):761–764. doi:10.1126/science.233.4765.761
- McCorkle, D.C., Martin, P.A., Lea, D.W., and Klinkhammer, G.P., 1995. Evidence of a dissolution effect on benthic foraminiferal shell chemistry: $\delta^{13}\text{C}$, Cd/Ca, Ba/Ca, and Sr/Ca results from the Ontong Java Plateau. *Paleoceanography*, 10(4):699–714. doi:10.1029/95PA01427
- McIntyre, A., and Bé, A.W.H., 1967. Modern coccolithophoridae of the Atlantic Ocean—I. Placoliths and cyrtoliths. *Deep-Sea Res., Part A*, 14:561–597.
- McIntyre, A., Bé, A.W.H., and Roche, M.B., 1970. Modern Pacific coccolithophorida: a paleontological thermometer. *Trans. N.Y. Acad. Sci.*, 32(6):720–731.

- Minas, H.J., Minas, M., and Packard, T.T., 1986. Productivity in upwelling areas deduced from hydrographic and chemical fields. *Limnol. Oceanogr.*, 31:1180–1204.
- Müller, P.J., and Suess, E., 1979. Productivity, sedimentation rate, and sedimentary organic matter in the oceans—I. Organic carbon preservation. *Deep-Sea Res., Part A*, 26(12):1347–1362. doi:10.1016/0198-0149(79)90003-7
- Murray, J.W., Barber, R.T., Roman, M.R., Bacon, M.P., and Feely, R.A., 1994. Physical and biological controls on carbon cycling in the equatorial Pacific. *Science*, 266(5182):58–65. doi:10.1126/science.266.5182.58
- Mutti, M., 2000. Bulk $\delta^{18}\text{O}$ and $\delta^{13}\text{C}$ records from Site 999, Colombian Basin, and Site 1000, Nicaraguan Rise (latest Oligocene to middle Miocene): diagenesis, link to sediment parameters, and paleoceanography. In Leckie, R.M., Sigurdsson, H., Acton, G.D., and Draper, G. (Eds.), *Proc. ODP, Sci. Results*, 165: College Station, TX (Ocean Drilling Program), 275–283. doi:10.2973/odp.proc.sr.165.016.2000
- Nishimura, S., and Suparka, S., 1997. Tectonic approach to the Neogene evolution of Pacific-Indian Ocean seaways. *Tectonophysics*, 281(1–2):1–16. doi:10.1016/S0040-1951(97)00155-8
- Paytan, A., Kastner, M., and Chavez, F.P., 1996. Glacial to interglacial fluctuations in productivity in the equatorial Pacific as indicated by marine barite. *Science*, 274(5291):1355–1357. doi:10.1126/science.274.5291.1355
- Peters, J.L., Murray, R.W., Sparks, J.W., and Coleman, D.S., 2000. Terrigenous matter and dispersed ash in sediment from the Caribbean Sea: results from Leg 165. In Leckie, R.M., Sigurdsson, H., Acton, G.D., and Draper, G. (Eds.), *Proc. ODP, Sci. Results*, 165: College Station, TX (Ocean Drilling Program), 115–124. doi:10.2973/odp.proc.sr.165.003.2000
- Peterson, L.C., Murray, D.W., Ehrmann, W.U., and Hempel, P., 1992. Cenozoic carbonate accumulation and compensation depth changes in the Indian Ocean. In Duncan, R.A., Rea, D.K., Kidd, R.B., von Rad, U., and Weissel, J.K. (Eds.), *Synthesis of Results from Scientific Drilling in the Indian Ocean*. Geophys. Monogr., 70:311–333.
- Pettke, T., Halliday, A.N., and Rea, D.K., 2002. Cenozoic evolution of Asian climate and sources of Pacific seawater Pb and Nd derived from eolian dust of sediment core LL44-GPC3. *Paleoceanography*, 17(3):1031. doi:10.1029/2001PA000673
- Raffi, I., and Flores, J.-A., 1995. Pleistocene through Miocene calcareous nannofossils from eastern equatorial Pacific Ocean (Leg 138). In Pisias, N.G., Mayer, L.A., Janecek, T.R., Palmer-Julson, A., and van Andel, T.H. (Eds.), *Proc. ODP, Sci. Results*, 138: College Station, TX (Ocean Drilling Program), 233–286. doi:10.2973/odp.proc.sr.138.112.1995
- Rea, D.K., 1994. The paleoclimatic record provided by eolian deposition in the deep sea: the geologic history of wind. *Rev. Geophys.*, 32(2):159–196. doi:10.1029/93RG03257
- Rea, D.K., and Bloomstine, M.K., 1986. Neogene history of the South Pacific tradewinds: evidence for hemispherical asymmetry of atmospheric circulation. *Palaeogeogr., Palaeoclimatol., Palaeoecol.*, 55(1):55–64. doi:10.1016/0031-0182(86)90137-9
- Rea, D.K., Pisias, N.G., and Newberry, T., 1991. Late Pleistocene paleoclimatology of the central equatorial Pacific: flux patterns of biogenic sediments. *Paleoceanography*, 6(2):227–244.
- Romine, K., and Lombardi, G., 1985. Evolution of Pacific circulation in the Miocene: radiolarian evidence from DSDP Site 289. In Kennett, J.P. (Ed.), *The Miocene Ocean: Paleoceanography and Biogeography*. Mem.—Geol. Soc. Am., 163:273–290.
- Roth, J.M., Droxler, A.W., and Kameo, K., 2000. The Caribbean carbonate crash at the middle to late Miocene transition: linkage to the establishment of the modern global ocean conveyor. In Leckie, R.M., Sigurdsson, H., Acton, G.D., and Draper, G. (Eds.), *Proc. ODP, Sci. Results*, 165: College Station, TX (Ocean Drilling Program), 249–273. doi:10.2973/odp.proc.sr.165.013.2000
- Schlanger, S.O., and Douglas, R.G., 1974. The pelagic ooze-chalk-limestone transition and its implication for marine stratigraphy. In Hsü, K.J., and Jenkyns, H.C. (Eds.), *Pelagic Sediments: On Land and Under the Sea*. Spec. Publ.—Int. Assoc. Sedimentol., 1:117–148.

- Schrag, D.P., DePaolo, D.J., and Richter, F.M., 1992. Oxygen isotope exchange in a two-layer model of oceanic crust. *Earth Planet. Sci. Lett.*, 111(2–4):305–317. doi:10.1016/0012-821X(92)90186-Y
- Schrag, D.P., DePaolo, D.J., and Richter, F.M., 1995. Reconstructing past sea surface temperatures: correcting for diagenesis of bulk marine carbonate. *Geochim. Cosmochim. Acta*, 59(11):2265–2278. doi:10.1016/0016-7037(95)00105-9
- Sen, A., Kendall, C.G.St.C., and Levine, P., 1999. Combining a computer simulation and eustatic events to date seismic sequence boundaries: a case study of the Neogene of the Bahamas. *Sediment. Geol.*, 125(1–2):47–59. doi:10.1016/S0037-0738(98)00147-X
- Shackleton, N.J., and Hall, M.A., 1984. Carbon isotope data from Leg 74 sediments. In Moore, T.C., Jr., Rabinowitz, P.D., et al., *Init. Repts. DSDP*, 74: Washington, DC (U.S. Govt. Printing Office), 613–619.
- Shackleton, N.J., and Hall, M.A., 1995. Stable isotope records in bulk sediments (Leg 138). In Pisias, N.G., Mayer, L.A., Janecek, T.R., Palmer-Julson, A., and van Andel, T.H. (Eds.), *Proc. ODP, Sci. Results*, 138: College Station, TX (Ocean Drilling Program), 797–805. doi:10.2973/odp.proc.sr.138.150.1995
- Shackleton, N.J., Hall, M.A., Pate, D., Meynadier, L., and Valet, J.-P., 1993. High-resolution stable isotope stratigraphy from bulk sediment. *Paleoceanography*, 8:141–148.
- Shackleton, N.J., and Kennett, J.P., 1975. Paleotemperature history of the Cenozoic and the initiation of Antarctic glaciation: oxygen and carbon isotope analyses in DSDP Sites 277, 279, and 281. In Kennett, J.P., Houtz, R.E., et al., *Init. Repts. DSDP*, 29: Washington, DC (U.S. Govt. Printing Office), 743–755.
- Shipboard Scientific Party, 2002. Leg 199 summary. In Lyle, M., Wilson, P.A., Janecek, T.R., et al., *Proc. ODP, Init. Repts.*, 199: College Station, TX (Ocean Drilling Program), 1–87. doi:10.2973/odp.proc.ir.199.101.2002
- Shipboard Scientific Party, 2003. Site 1256. In Wilson, D.S., Teagle, D.A.H., Acton, G.D., et al., *Proc. ODP, Init. Repts.*, 206: College Station, TX (Ocean Drilling Program), 1–396. doi:10.2973/odp.proc.ir.206.103.2003
- Sigurdsson, H., Kelley, S., Leckie, R.M., Carey, S., Bralower, T., and King, J., 2000. History of circum-Caribbean explosive volcanism: $^{40}\text{Ar}/^{39}\text{Ar}$ dating of tephra layers. In Leckie, R.M., Sigurdsson, H., Acton, G.D., and Draper, G. (Eds.), *Proc. ODP, Sci. Results*, 165: College Station, TX (Ocean Drilling Program), 299–314. doi:10.2973/odp.proc.sr.165.021.2000
- Snoeckx, H., Rea, D.K., Jones, C.E., and Ingram, B.L., 1995. Eolian and silica deposition in the central North Pacific: results from Sites 885/886. In Rea, D.K., Basov, I.A., Scholl, D.W., and Allan, J.F. (Eds.), *Proc. ODP, Sci. Results*, 145: College Station, TX (Ocean Drilling Program), 219–230. doi:10.2973/odp.proc.sr.145.123.1995
- Spero, H.J., Bijma, J., Lea, D.W., and Bemis, B.E., 1997. Effect of seawater carbonate concentration on foraminiferal carbon and oxygen isotopes. *Nature (London, U. K.)*, 390(6659):497–500. doi:10.1038/37333
- Stoll, H.M., 2005. Limited range of interspecific vital effects in coccolith stable isotopic records during the Paleocene–Eocene Thermal Maximum. *Paleoceanography*, 20(1):PA1007. doi:10.1029/2004PA001046
- Talley, L.D., and Roemmich, D., 1991. Map Set for “Joseph L. Reid: a tribute in recognition of 40 years of contributions to oceanography.” *Deep-Sea Res.*, 38(Suppl.):1A.
- Tappan, H., 1968. Primary production, isotopes, extinctions and the atmosphere. *Palaeogeogr., Palaeoclimatol., Palaeoecol.*, 4(3):187–210. doi:10.1016/0031-0182(68)90047-3
- Theyer, F., Mayer, L.A., Barron, J.A., and Thomas, E., 1985. The equatorial Pacific high-productivity belt: elements for a synthesis of Deep Sea Drilling Project Leg 85 results. In Mayer, L., Theyer, F., Thomas, E., et al., *Init. Repts. DSDP*, 85: Washington, DC (U.S. Govt. Printing Office), 971–985.
- Tsuchi, R., 1997. Marine climatic responses to Neogene tectonics of the Pacific Ocean seaways. *Tectonophysics*, 281(1–2):113–124. doi:10.1016/S0040-1951(97)00163-7

- van Andel, T.H., Heath, G.R., and Moore, T.C., Jr., 1975. *Cenozoic History and Paleooceanography of the Central Equatorial Pacific Ocean: A Regional Synthesis of Deep Sea Drilling Project Data*. Mem.—Geol. Soc. Am., 143.
- Vincent, E., Killingley, J.S., and Berger, W.H., 1985. Miocene oxygen and carbon isotope stratigraphy of the tropical Indian Ocean. In Kennett, J.P. (Ed.), *The Miocene Ocean: Paleooceanography and Biogeography*. Mem.—Geol. Soc. Am., 163:103–130.
- Vossepoel, F.C., Reynolds, W.R., and Miller, L., 1999. Use of sea level observations to estimate salinity variability in the tropical Pacific. *J. Atmos. Oceanic Technol.*, 16(10):1401–1415. doi:10.1175/1520-0426(1999)016<1401:UOSLOT>2.0.CO;2
- Walsh, I., Dymond, J., and Collier, R., 1988. Rates of recycling of biogenic components of settling particles in the ocean derived from sediment trap experiments. *Deep-Sea Res., Part A*, 35(1):43–58. doi:10.1016/0198-0149(88)90056-8
- Weber, M.E., and Pisias, N.G., 1999. Spatial and temporal distribution of biogenic carbonate and opal in deep-sea sediments from the eastern equatorial Pacific: implications for ocean history since 1.3 Ma. *Earth Planet. Sci. Lett.*, 174(1–2):59–73. doi:10.1016/S0012-821X(99)00248-4
- Weinberg, E., 1989. Cellular regulation of iron assimilation. *Q. Rev. Biol.*, 64(3):261–289.
- Westerhold, T., Bickert, T., and Paulsen, H., 2003. History of carbonate and terrigenous sedimentation at South Atlantic ODP Site 1092 for the last 14 Ma. *Geophys. Res. Abstr.*, 5:02311.
- Wilson, D.S., 1996. Fastest known spreading on the Miocene Cocos–Pacific plate boundary. *Geophys. Res. Lett.*, 23(21):3003–3006. doi:10.1029/96GL02893
- Wise, S.W., 1977. Chalk formation: early diagenesis. In Anderson, N.R., and Malahoff, A. (Eds.), *The Fate of Fossil Fuel CO₂ in the Oceans*: New York (Plenum Press), 717–739.
- Wise, S.W., 2003. Carbonate compensation depth. In Middleton, G.V. (Ed.), *Encyclopedia of Earth Sciences Series: Encyclopedia of Sediments and Sedimentary Rocks*: Amsterdam (Kluwer Academic Press), 88–89.
- Woodruff, F., and Savin, S.M., 1991. Mid-Miocene isotope stratigraphy in the deep sea: high resolution correlations, paleoclimatic cycles, and sediment preservation. *Paleooceanography*, 6:755–806.
- Wyrcki, K., 1974. Equatorial currents in the Pacific 1950 to 1970 and their relations to the trade winds. *J. Phys. Oceanogr.*, 4(3):372–380. doi:10.1175/1520-0485(1974)004<0372:ECITPT>2.0.CO;2
- Wyrcki, K., 1981. An estimate of equatorial upwelling in the Pacific. *J. Phys. Oceanogr.*, 11(9):1205–1214. doi:10.1175/1520-0485(1981)011<1205:AEOEUI>2.0.CO;2
- Zachos, J., Pagani, M., Sloan, L., Thomas, E., and Billups, K., 2001. Trends, rhythms, and aberrations in global climate 65 Ma to present. *Science*, 292(5517):686–693. doi:10.1126/science.1059412

Figure F1. Locations of Site 1256 and other ODP/DSDP sites with major world surface currents. Dashed arrows = Equatorial Undercurrent in the Pacific Ocean, solid line = annual shift of the Intertropical Convergence Zone in July, dashed line = annual shift of the Intertropical Convergence Zone in January, gray arrow = Equatorial Countercurrent.

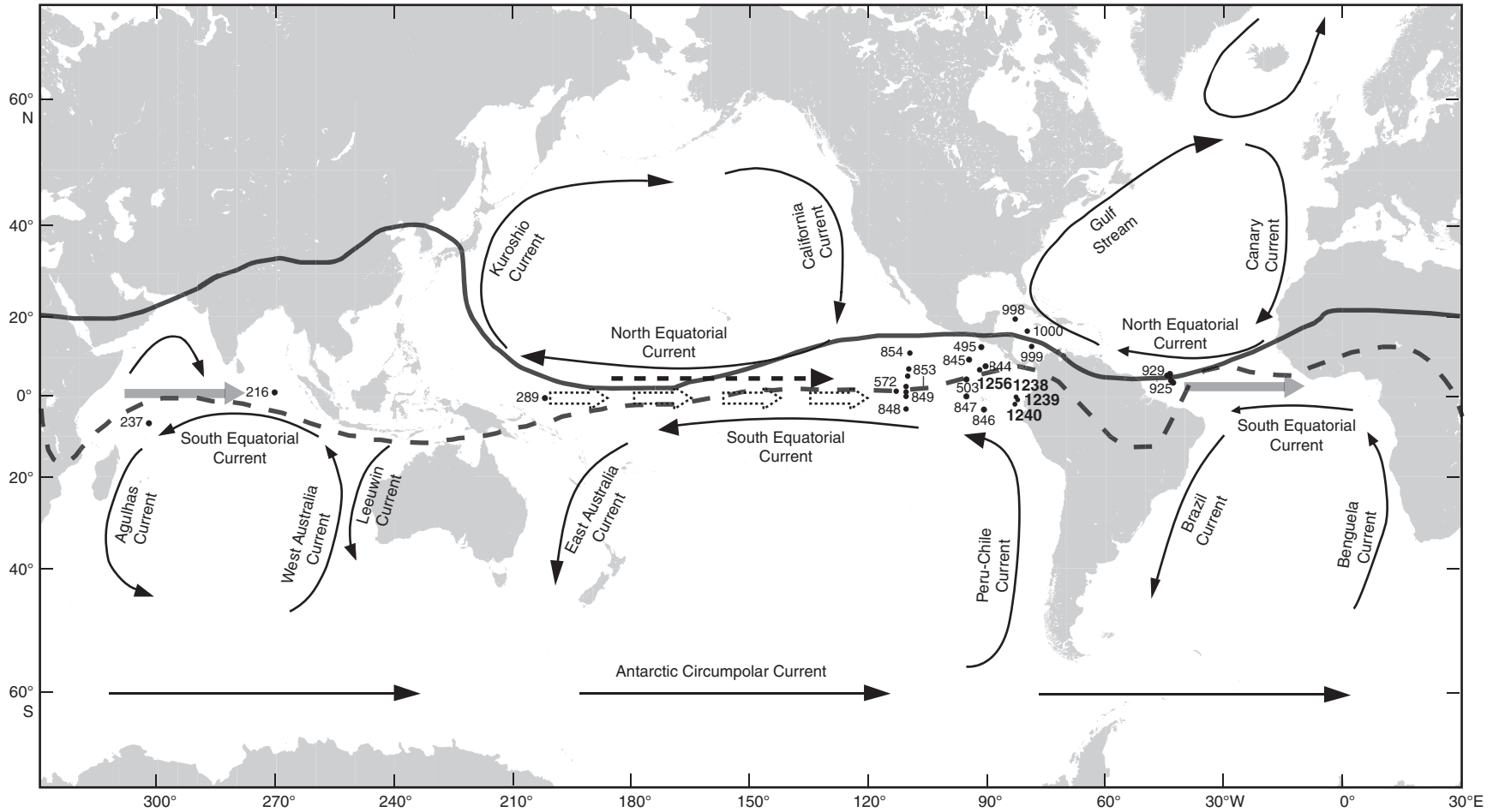


Figure F2. (A) Variations of carbonate mass accumulation rates (MARs) and stable oxygen and carbon isotopes in the studied interval, and (B) the correlation among them. Gray shading = critical interval spanning the carbonate crash. PDB = Peedee belemnite.

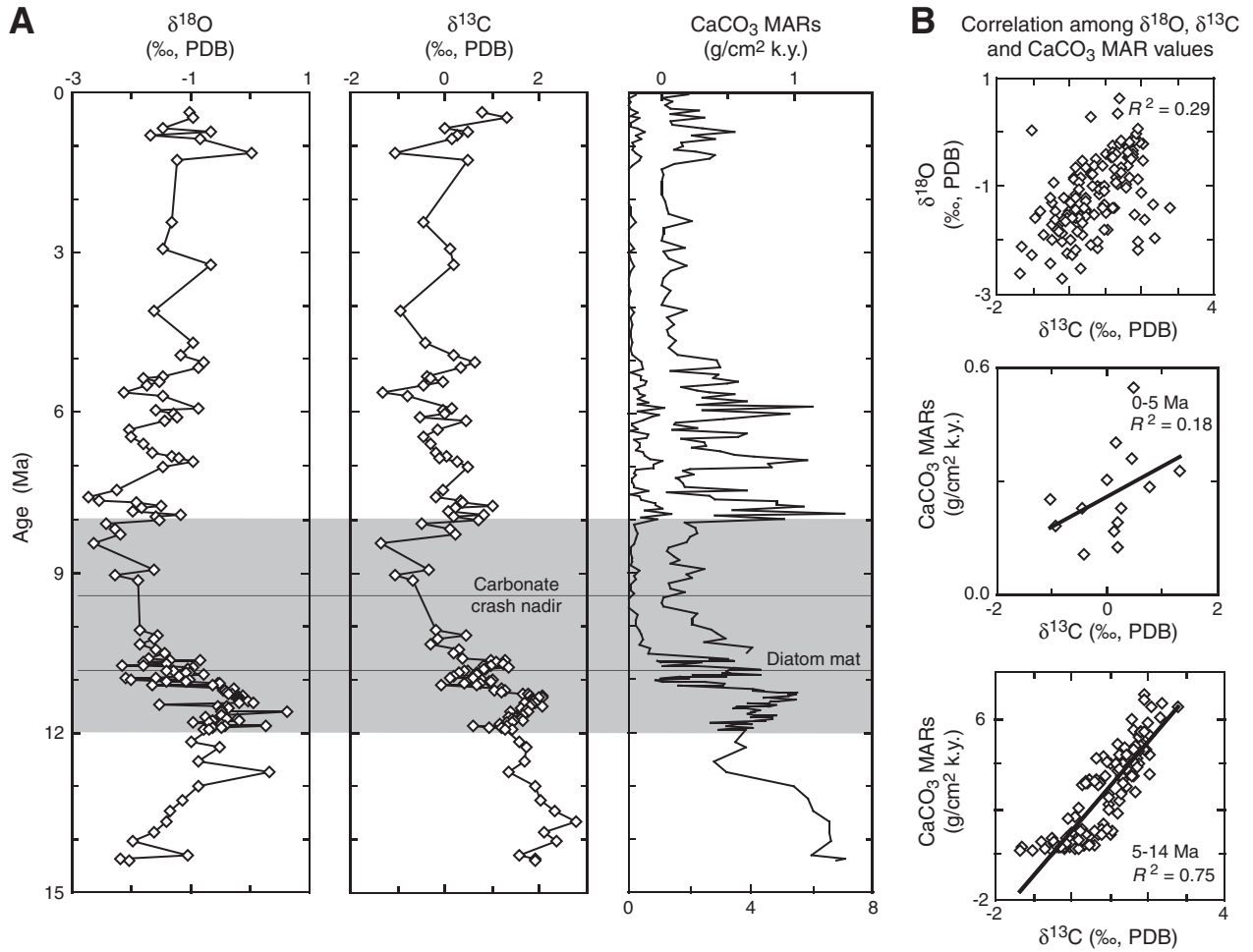


Figure F3. Relationship of mass accumulation rates between bulk sediments and the main sedimentary components (from Jiang and Wise, this volume).

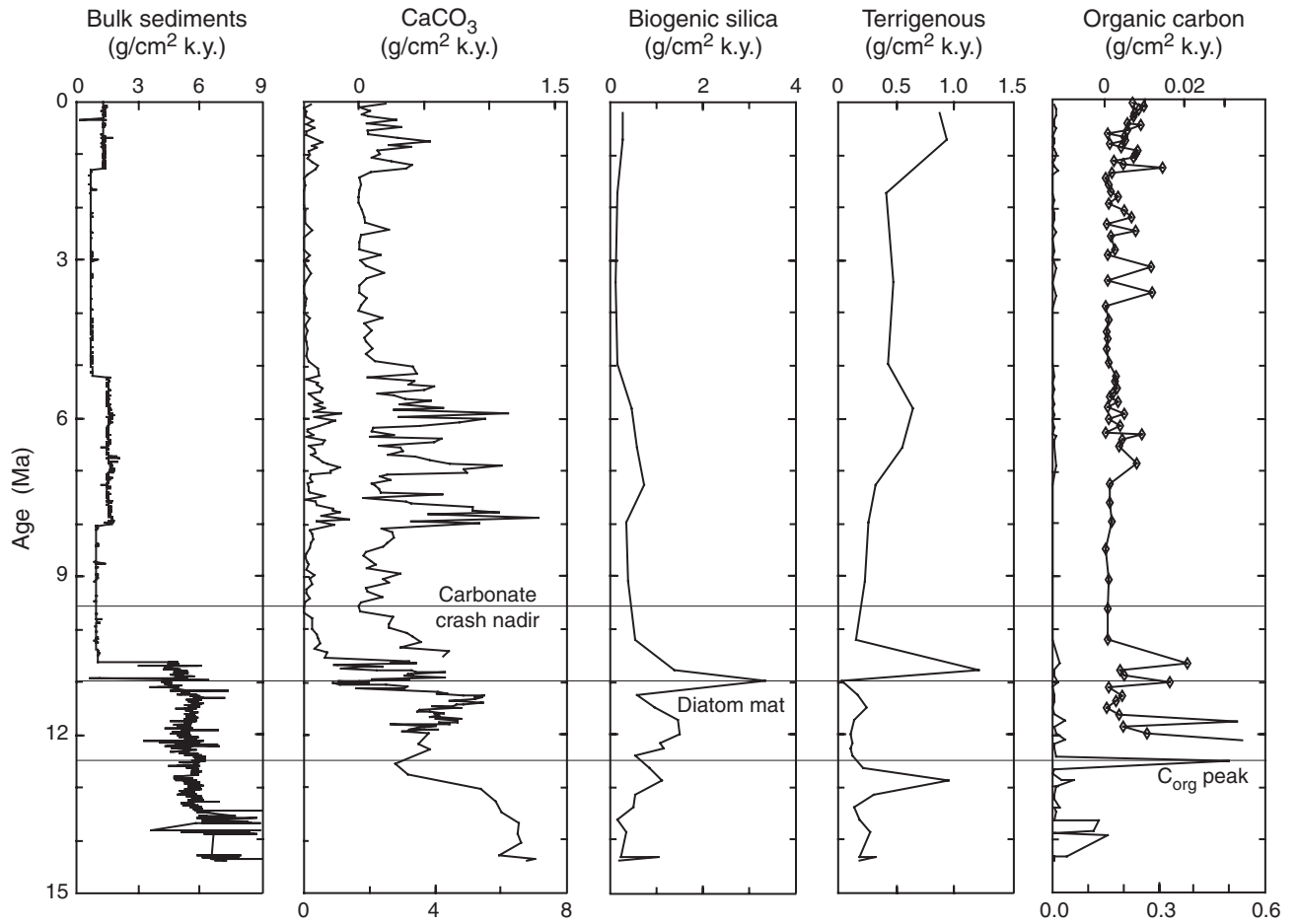


Figure F4. CaCO_3 and volcanic ash mass accumulation rates (MARs) from ODP Leg 165. All data are from Peters et al. (2000). Note the close correlation between MARs of CaCO_3 and volcanic ash at each site.

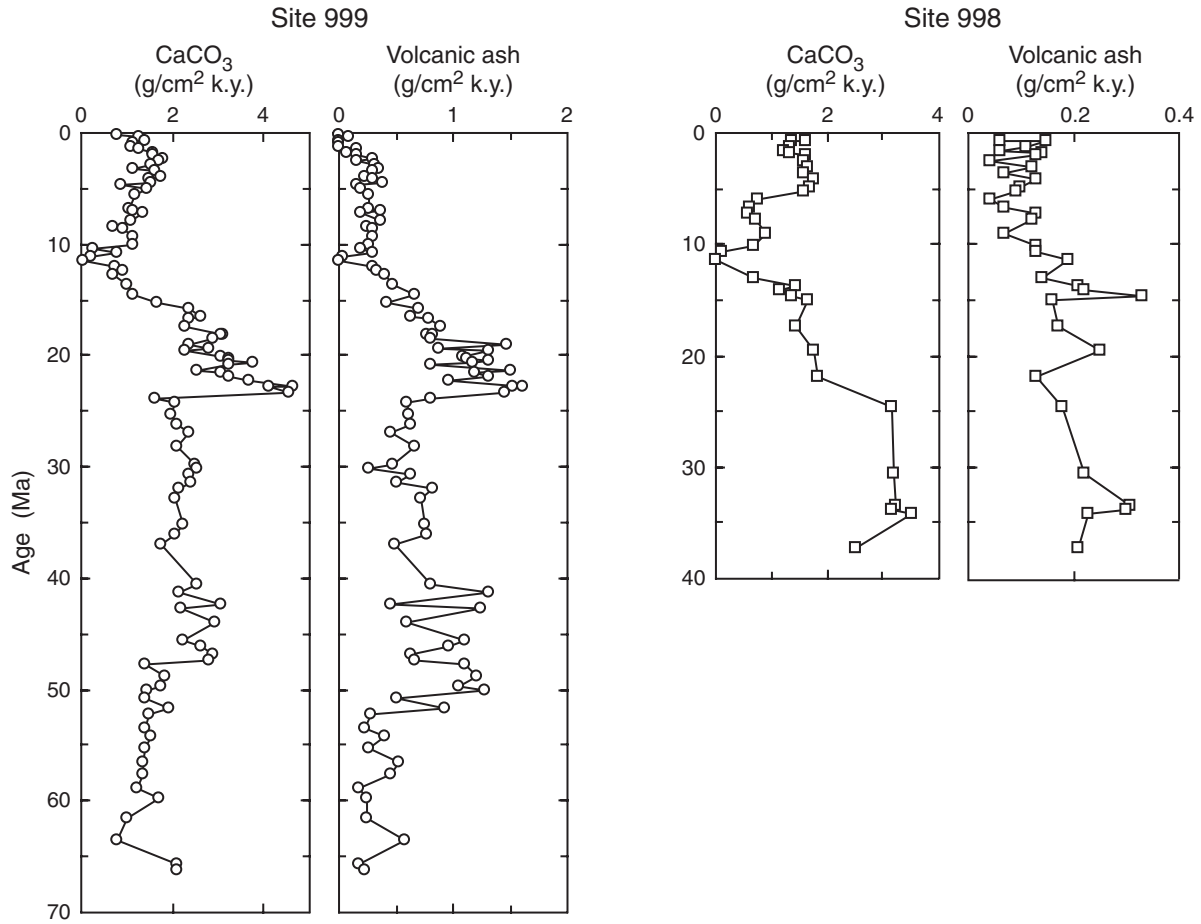


Figure F5. $\delta^{13}\text{C}$ of the (A) modern western Atlantic, (B) eastern Pacific, and (C) circumpolar Antarctic (from Kroopnick, 1985).

